Accepted Manuscript

Modulated diamond cutting for the generation of complicated micro/nanofluidic channels

Zhiwei Zhu, Suet To, Zhen Tong, Zhuoxuan Zhuang, Xiangqian Jiang

PII: S0141-6359(18)30285-X

DOI: https://doi.org/10.1016/j.precisioneng.2018.11.008

Reference: PRE 6877

To appear in: *Precision Engineering*

Received Date: 5 May 2018

Revised Date: 30 August 2018

Accepted Date: 20 November 2018

Please cite this article as: Zhu Z, To S, Tong Z, Zhuang Z, Jiang X, Modulated diamond cutting for the generation of complicated micro/nanofluidic channels, *Precision Engineering* (2018), doi: https://doi.org/10.1016/j.precisioneng.2018.11.008.

Modulated diamond cutting for the generation of complicated micro/nanofluidic channels

Zhiwei Zhu[a], Suet To[b,†], Zhen Tong[c], Zhuoxuan Zhuang[b] and Xiangqian Jiang[c]

a. School of Mechanical Engineering, Nanjing University of Science and Technology, Nanjing, J.S. 210094, China

b. State Key Laboratory of Ultra-precision Machining Technology, Department of Industrial and Systems Engineering, The Hong Kong Polytechnic University, Kowloon, Hong Kong SAR, China

c. Centre for Precision Technologies, University of Huddersfield, Huddersfield, UK HD1 3DH

†. Corresponding author: sandy.to@polyu.edu.hk

Abstract

A novel modulated diamond cutting (MDC) technique is proposed for the generation of complicated micro/nanofluidic channels. The MDC adopts a turning configuration through a four-axis ultra-precision diamond lathe, a motion modulation based milling operation is introduced by extending the virtual spindle technique. This unique principle makes the MDC more suitable to generate micro/nanofluidic channels through compromising certain inherent advantages of both diamond turning and milling. Moreover, taking advantage of axial servo motion modulation as well as tool mark modulation using the re-cutting effect, complicated channels can be effectively generated having spatially-varying shapes as well as hierarchical micro/nanostructures. Through both numerical simulation and experimental cutting, capability and outperformance of the MDC are demonstrated well. The result suggests that the MDC is capable to generate ultra-smooth channel surfaces with complicated shapes and superimposed surface nanostructures, exhibiting significant superiority for the generation of micro/nanofluidic channels with high flexibility, high efficiency, and high universality.

Keywords: Modulated diamond cutting, micro/nanofluidic channels, tool mark modulation, hierarchically structured surface.

1. Introduction

Micro/nanofluidic channels with feature dimensions ranging from tens of nanometres to tens of micrometres are essential for precise manipulation of fluids in picoliters or even femtoliters scale [1]. It is now attracting ever-increasing attention in a variety of fields, including biological analysis [1], chemical synthesis [2], and plasmofluidics [3], to mention a few. It was reported that the channels with spatially-varying shapes can provide high flexibility for the tuning of the micro/nanofluidic transport behaviour [4, 5]. Moreover, channels with superimposed surface nanostructures can lead to unusual physics or geometry governed fluidic effects, significantly extending novel capability and performance of micro/nanofluidic devices and applications [6].

Currently, lithography based fabrication methods (e.g., photolithography, laser direct-write, nanoimprinting, and electron beam lithography) are dominant for the generation of micro/nanofluidic channels [1, 5, 6].A detailed review of recent lithography based fabrication methods can be found in Ref. [7] for the generation of these related channels. In general, most of these techniques may suffer from: i) laborious multiple processes to create three-dimensional (3-D) shapes, especially with superimposition of surface nanostructures [8, 9]; ii) limited capability to fabricate continuously curved channels with ultra-high dimensional accuracy and surface quality; and iii) low mass production rate of the channels [10].

More recently, the bottom-up based 3-D printing technique was recommended for the generation of microfluidic channels. Although it is highly efficient for fast prototyping, most of the additive methods may suffer from low resolution and rough channel surfaces, reducing its appeal for micro/nanofluidic applications [11–14]. Micro-milling which belongs to top-down based mechanical machining was also introduced to rapidly generate microfluidic channels, mainly attributed to the unique advantages of high production rate, low cost, and universality of processed materials [10, 15]. However, there are challenges to generate complex channels in the micro/nanoscales

which mainly due to the limited geometrical shape of micro-milling tools as well as the inherent kinematics of milling operations. Moreover, it remains impossible for the developed micro-milling techniques to create hierarchical surfaces featuring superimposed secondary nanostructures on the basic curved walls of micro-channels. To decrease the feature dimensions, atomic force microscope (AFM) based nano-milling with controlled normal cutting force was developed to generate channels in the nanoscale, which can achieve sub-100 nm lateral resolution and sub-10 nm vertical resolution [16–18]. In general, it employs a sharp AFM tip on a flexible cantilever to fabricate nanoscale features at the expense of relatively low efficiency, low accuracy, and high tip wear rate, significantly restricting its application for high throughput requirements [16].

Compared with micro-milling, diamond turning adopts natural single crystal diamond tools with controllable nose radius from millimetres down to dozens of nanometres, making it ideal to fabricate micro/nanostructured surfaces [19–21]. Additional oscillations in the turning further extends its capability for the generation of complicated surfaces with high flexibility and high quality [22]. Although diamond turning exhibits complementary functions to micro-milling, the inherent spiral trajectory makes it extremely difficult to generate micro/nanofluidic channels with spatially-varying shapes, especially for the ones with superimposed functional nanostructures. In principle, an ideal solution for creating a complicated channel is to take a rotating tool along the channel trend to remove bulk materials, just as micro-milling does. In addition, ultra-fine oscillations of the diamond tools with controllable shapes in tool servo based turning are expected to gain the capability for complicated channel generation with high complexity, high flexibility, and high efficiency. Considering these requirements, an alternative rotary vibration based diamond cutting is promising in terms of rotary tool and fast spatial oscillations [23, 24]. However, with respect to the state-of-the-art rotary vibration based cutting [23, 24], the fixed rotation radius between the cutting edge and spindle axis may limit its flexibility on machining channels with spatially-varying

width.

Motivated by this, a novel modulated diamond cutting (MDC) technique which retains indispensable features of both tool servo based turning and micro-milling is proposed to fabricate micro/nanofluidic channels. The main contributions of this study can be summarized as follows:

- Propose to employ single point diamond cutting technique for the generation of micro/nanofluidic channels with spatially-varying shapes as well as with superimposed surface nanostructures, which are often difficult for the state-of-the-art manufacturing methods to achieve.
- Propose to synthesize fundamental concepts of conventional diamond turning and micro-milling through generating modulated motions, and the accordingly formed MDC technique greatly extends the machining capability of both turning and micro-milling processes.
- The developed MDC technique outperforms the current manufacturing methods in terms of the flexibility to shape complexity, the generality to processed materials, and the efficiency to mass production rate, providing more freedoms for micro/nanofluidic device design.

2. Principle of modulated diamond cutting

2.1. Motion modulation for basic channel generation

The MDC technique adopts a basic configuration of a four-axis ultra-precision lathe as shown in Fig. 1, and an enlarged view of the interaction of the diamond tool and sample is also illustrated at the upper right corner in Fig. 1. The $o_m - x_m y_m z_m$ and $o_w - x_w y_w z_w$ are the fixed Cartesian coordinate systems of the lathe and workpiece, respectively. The two coordinate systems initially coincide with each other, and the $o_m z_m$ ($o_w z_w$) axis coincides with the spindle axis. The difference is that the $o_w - x_w y_w z_w$ system will rotate with the spindle. A diamond turning tool is fixed on a tool holder installed on the z_m-axial slide, and through a vacuum chuck, the workpiece is attached on the aero-bearing spindle with rotation axis being parallel to the z_m-axis.

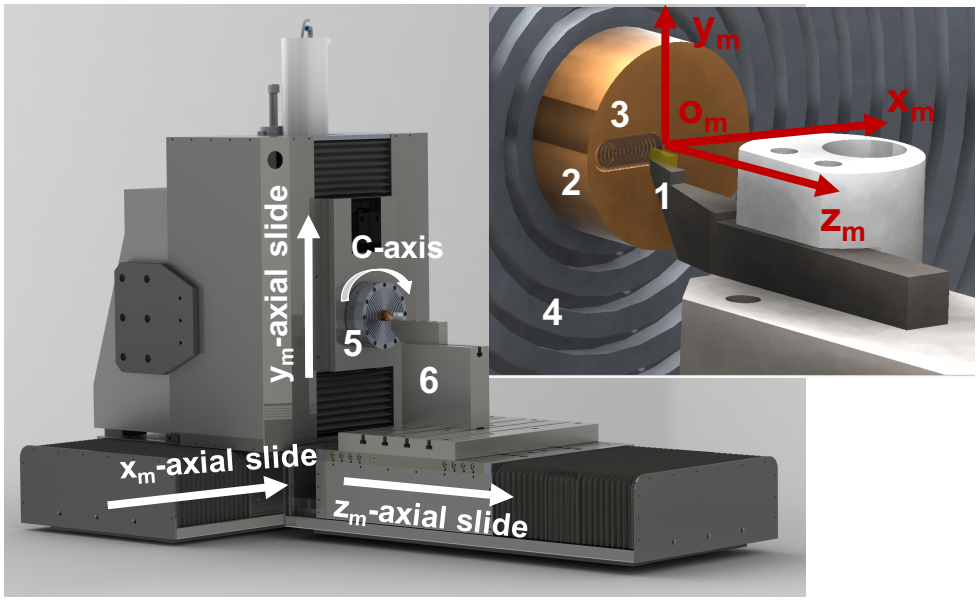

Figure 1: System configuration for micro/nanofluidic channel generation, 1 diamond tool, 2 sample, 3 generated channel, 4 vacuum chuck, 5 spindle, 6 tool holder.

A projected two-dimensional (2-D) schematic of a desired channel and the relative cutting kinematics of the MDC is illustrated in Fig. 2. With respect to an arbitrary point $o_c(k)$ in the central axis of the channel, the distance relative to the spindle axis and the corresponding polar angle are ρ_k and θ_k, respectively. During cutting, point o_c will be set to move along the central line of the micro/nanofluidic channel with a feeding speed of f per revolution of the spindle. If the rotational speed of the spindle is denoted by S, the polar angle can be obtained with respect to time t_k as $\theta_k = \frac{\pi S t_k}{30}$.

Considering the trend of the channel, the relative position between the two successive points $o_c(k+1)$ and $o_c(k)$ can be expressed by

$$x_c(k+1) = (\rho_k + \delta)\cos(\theta_k + \vartheta) \tag{1}$$

$$y_c(k+1) = (\rho_k + \delta)\sin(\theta_k + \vartheta) \tag{2}$$

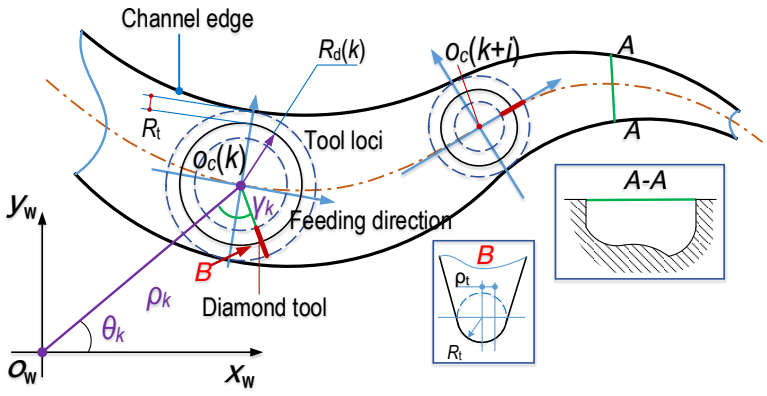

Figure 2: Schematic of cutting kinematics for micro/nanofluidic channel generation, where $o_c(k)$ and $o_c(k+i)$ are the k-th and $(k+i)$-th point (corresponding to time t_k and t_{k+i}) in the central axis of the channel.

where δ and ϑ are the incremental distance and angle of the point $o_c(k+1)$ relative to the point $o_c(k)$ in the $o_w - x_w y_w z_w$ system, respectively.

To satisfy the requirement for the usage of a rotating tool to move along the channel trend, the following law should always be satisfied for any arbitrary k, δ and ϑ:

$$(x_t - x_c)^2 + (y_t - y_c)^2 \equiv R_d^2 \tag{3}$$

where (x_t, y_t) is the planar Cartesian coordinate of the cutter location point (CLP) in the $o_w - x_w y_w z_w$ system which is defined as the centre of the circular edge of the diamond tool, and R_d is the equivalent rotational radius defined as the distance between the CLP and point $o_c(k)$ at time t_k.

To guarantee effective cutting, the point o_c should be on the plane of the rake face of the tool. Considering that the rake face is horizontal in the machine tool system, CLPs of the diamond tool should satisfy $x_t = R_d + x_c$, and $y_t = y_c$. The relationship in Eq. (1) and Eq. (2) suggests that planar quasi-harmonic motions with the same frequency as the spindle and position dependent amplitude should be modulated on the tool to execute the desired rotational cutting. Moreover, the rotational

axes are controlled along the trending direction of the channel in the MDC. Considering the planar quasi-harmonic motions, the servo motion along the z_m-axial direction, and the spindle rotation, an ultra-precision lathe with the four axes being concurrently controlled is essentially required to implement the proposed MDC technique.

It is noteworthy that although the motion modulation based virtual spindle technique is employed to control the position of the rotational axis [22], the cutting method reported in [22] is essentially a turning process. In the MDC, continuous changing of the axis position with constant or channel shape determined rotational radius is adopted, which operates in a milling-like mode.

2.2. Motion modulation for complicated channel generation

Commonly, a micro/nanofluidic channel may have spatially-varying 3-D features in the micro-scale and even nano-scale. With the relative position between the diamond tool and workpiece shown in Fig. 2, the coordinate of an arbitrary point at the tool edge in the $o_w - x_w y_w z_w$ system can be expressed by

$$\begin{bmatrix} x_p(k) \\ y_p(k) \\ z_p(k) \end{bmatrix} = \begin{bmatrix} \rho_k \cos\theta_k \\ \rho_k \sin\theta_k \\ 0 \end{bmatrix} + \begin{bmatrix} (R_d + \rho_t)\cos\gamma_k \\ (R_d + \rho_t)\sin\gamma_k \\ z_m(k) + g(\rho_t) \end{bmatrix} \begin{bmatrix} -\cos\theta_k & -\sin\theta_k & 0 \\ \sin\theta_k & -\cos\theta_k & 0 \\ 0 & 0 & 1 \end{bmatrix} \tag{4}$$

where $z_m(k)$ is the z_m-axial servo motion, $g(\cdot)$ is the function relating the radial position $\rho_t \in [-R_t, R_t]$ and the corresponding profile of the tool edge [22], and γ_k is an included angle as shown in Fig. 2.

Assume the bottom surface of the designed channel can be mathematically expressed by $S(x_w, y_w)$ in the $o_w - x_w y_w z_w$ system, the required z_m-axial servo motion corresponding to this bottom surface can be obtained by:

$$z_m(k) = \min\left\{ g(\rho_t) - S\left[x_p(k), y_p(k)\right] > 0 \right\}, \ \forall \rho_t \tag{5}$$

Since the desired channel is created by the swept motion of the tool relative to the workpiece, channel shapes can be varied by controlling the position of the tool edge as described in Eq. (4). Besides the z_m-axial motion, the transient radius R_d can also be tuned in real time to efficiently adapt to width variation of the channel as illustrated in Fig. 2 ($A - A$).

2.3. Tool mark modulation for hierarchical channel generation

In general, there are inevitable tool marks on the machined surface in both turning and milling. By deliberately choosing the cutting parameters, shapes of the tool marks can be modulated to form desired textures for functionalization [25, 26]. Unlike the current tool mark control methods, the inherent re-cutting effects induced by the rotational cutting was adopted and superimposed on the tri-axial modulation motions in the MDC. Therefore, secondary nanostructures can be generated on bottom surfaces of the desired 3-D micro/nanofluidic channels.

To provide a more detailed illustration, the approximate relative cutting motion projected on the $o_w - x_w y_w$ plane is shown in Fig. 3. When the tool rotates from point TP' to TP, it executes forward cutting. After that, it will rotates from point TP to TP', leading to a re-cutting of the previously generated surface. This re-cutting effect can serves as possible tool mark modulation for surface texturing. As shown in Fig. 3, there are three types of structures formed by the tool marks on the machined surface, namely one hexagonal bulge in region I between point B and C, one ribbon bulge in region III, and a set of pyramid structures with variable dimensions in other regions (region II for example).

With respect to the ribbon bulge, the maximum height is highly dependent on the tool geometry, feedrate, and rotational radius. Assume that the feedrate per revolution is much smaller than the rotational radius ($f \ll R_d$), the maximum height can be approximately determined by

$$h_r = \frac{\rho_p}{|\rho_p|}\left(\sqrt{(\rho_p + R_t)^2 - 0.25d_{AB}^2} - 1\right) - \sqrt{R_t^2 - 0.25d_{AB}^2} \tag{6}$$

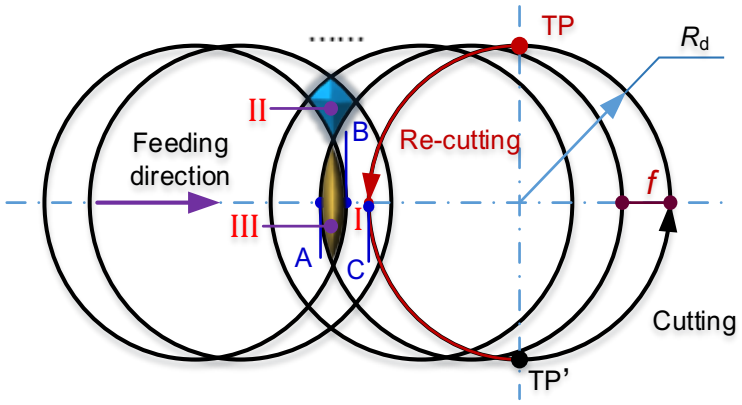

Figure 3: The projected cutting motion for tool mark modulation.

$$d_{AB} = \lceil 2R_d f^{-1} \rceil f - 2R_d \tag{7}$$

where ρ_p is the local curvature radius of the primary surface along the feeding direction, and d_{AB} is the distance between points A and B.

If the transient rotational diameter ($2R_d$) is an integral multiple of the feedrate f, point A will coincide with point B. At that time, the hexagonal bulge in region I will be transferred into the ribbon bulge in region III in Fig. 3, and the height of the newly formed ribbon bulge will reach its maximum with the value being obtained by setting $d_{AB} = d_{BC} = f$ in Eq. (6).

3. Experimental setup

The cutting experiments were conducted on a four-axis ultra-precision lathe from Moore Nanotechnology Corporation (350 FG, USA), and a single crystal diamond tool (Contour Fine Tooling Inc., UK) with nose radius of $R_t = 15.5$ μm was employed for material removal. Hardware configuration of the cutting system is photographically illustrated in Fig. 4(a), and a microscopic image of the employed diamond tool is shown in Fig. 4(b). The rake and flank angles of the tool were 0 and 7 degree, respectively. A cylinder brass sample (C-2600) fixed on a fixture was then attached to the spindle through a vacuum chuck. The sample was finely turned to be flat with surface roughness

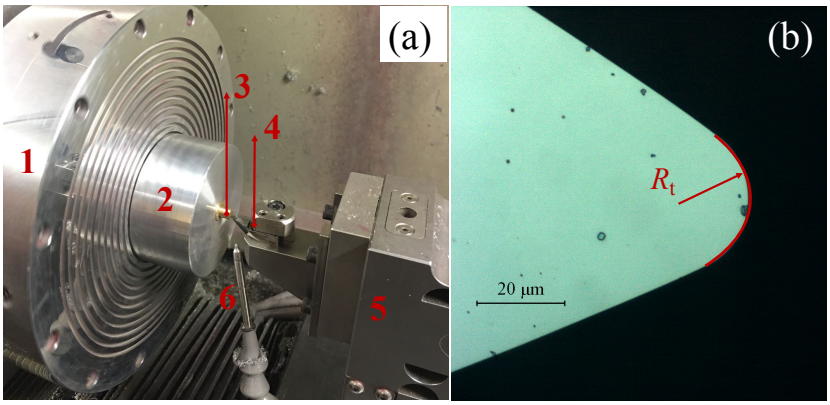

Figure 4: Photography of the machining system for micro/nanofluidic channels, (a) hardware configuration of the machining system, and (b) the microscopy image of the employed diamond tool, where 1 vacuum chuck, 2 fixture, 3 cylindrical sample, 4 diamond tool, 5 tool holder, 6 lubricant supplier; R_t denotes the nose radius of the diamond tool.

less than 10 nm before conducting the MDC operation. During cutting, the spindle speed was set around 30 rpm, and the lubricant oil was employed to facilitate material removal. Through close collaboration of the four-axial servo motions, complicated micro/nanofluidic channels can be generated well.

After cutting, the generated micro/nanofluidic channel was cleaned through alcohol with air blast to remove the attached segmented chips. The detailed 3-D topography of obtained channels was then captured through an optical surface profiler from Zygo Corporation (Nexview, USA), and the stitching strategy was employed to get surface data covering a relatively large area. After measurement, the obtained data was exported, analyzed, and depicted through a commercial software MATLAB.

4. Results and discussion

4.1. Generation of linear micro-channels

Without loss of generality, a micro/nanofluidic channel with freeform bottom surface mathematically described by $S(x_m, y_m) = A\cos(200\pi x_m) + A\sin(200\pi y_m)$ was generated to demonstrate the capability for the fabrication of micro/nanofluidic channels with complicated shapes. The am-

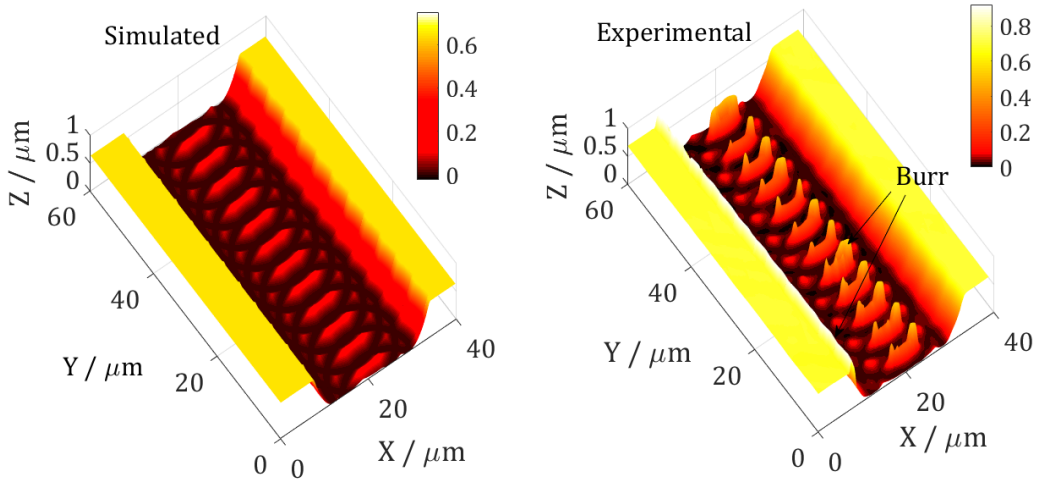

Figure 5: Numerically and experimentally generated micro/nanofluidic channel with spatially-varying shapes.

plitude for the surface is $A = 150$ nm, and the nominal depth-of-cut (DoC) is 0.6 μm which is also the height from the free surface to the valley point in the channel. In addition, the rotational radius and feedrate are set as $R_d = 9$ μm and $f = 2.5$ μm/rev, respectively. To verify the MDC technique, a surface generation model based on geometry computation is developed for numerical generation of the created channels. More details about the simulation model will be presented in our future work.

Figure 5 illustrates the numerically simulated as well as experimentally machined channel. The captured length is about 200 μm, which is double of the spatial periodicity of the desired surface $S(x_m, y_m)$. The obtained thinnest width of the channel is around 22.5 μm for both the simulated and experimental channels. It is slightly larger than the equivalent rotational diameter which might due to the round shape of the employed diamond tool. Moreover, the channel width is periodically varied which is jointly induced by the oscillation of the tool along the z_m-axis direction and the tool geometry. To decouple the width and depth variation of the channel, a square-edged rather than a round-edged tool is suggested. To actively control the spatially varying channel width, a modulation of the transient radius R_d is suggested which can be realized by tuning the amplitudes of the planar quasi-harmonic motions in real time. For example, using the same feedrate, a practical

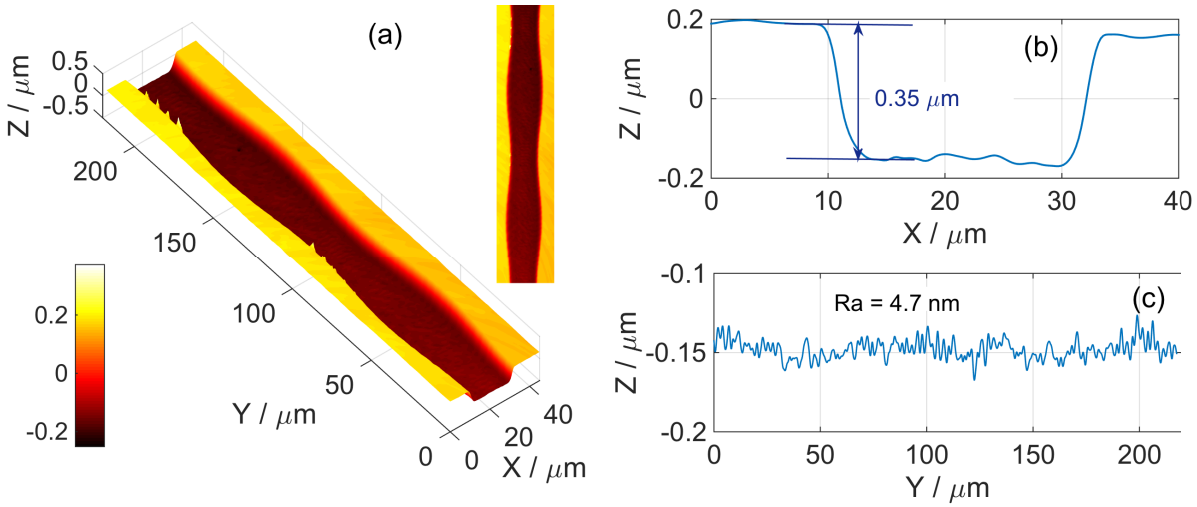

Figure 6: The practically generated micro/nanofluidic channel with harmonically varied width, (a) the 3-D topography of the channel, (b) the cross-sectional profile along the X direction at $Y = 100$ μm showing a channel depth of 0.35 μm, and (c) the cross-sectional profile along the Y direction at $X = 20$ μm.

3-D topography of a micro/nanofluidic channel is obtained in Fig. 6(a) with harmonically varied widths. The cross-sectional profile of the channel along the X direction exhibits a regular shape with a depth of 0.35 μm as shown in Fig. 6(b), and a ultra-smooth channel surface is also obtained along the Y direction with a roughness of Ra=4.7 nm (Fig. 6(c)).

By increasing the feedrate to be $f = 5$ μm/rev, a straight micro-channel with constant width and depth was also generated to have a set of superimposed surface nanostructures. The simulated and experimental channels are comparatively shown in Fig. 7. A good agreement between features of the theoretical and practical channels is observed. Theoretically, from Eq. (6) and Eq. (7), the maximum height of the ribbon structure in region III is estimated to be 32 nm, and the minimum height the hexagonal bulge in region I is estimated to be 73 nm. With a good accordance of the theoretical estimation, both the numerically and practically generated channels in Fig. 7 also suggest that the hexagonal bulge is the major type of surface nanostructures on the bottom of the channel. In addition, the pyramid nanostructure is also observed as that estimated in region II in Fig. 3.

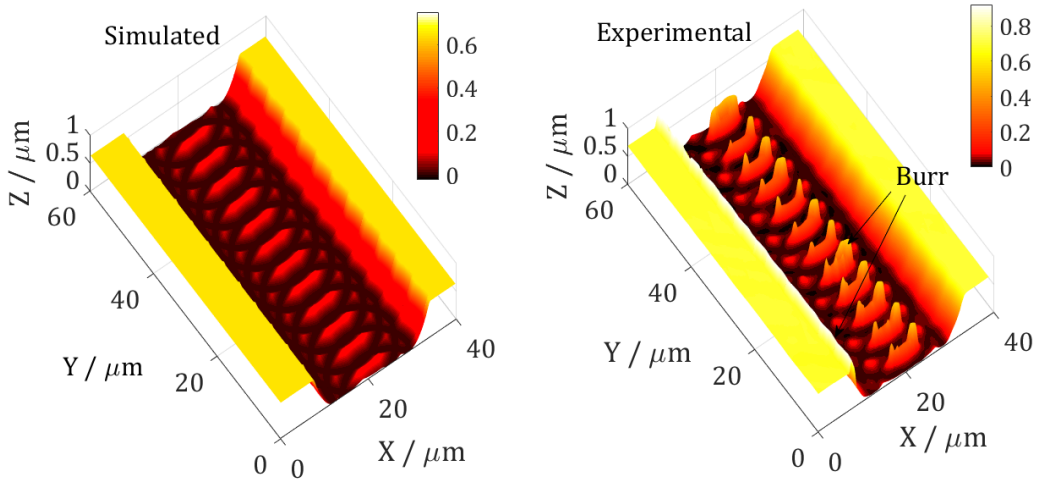

Figure 7: Numerically and experimentally generated micro/nanofluidic channel with superimposed surface nanostructures.

It is noteworthy that a large volume of burrs is found on the hexagonal bulge nanostructures as shown in Fig. 7, which may be a combination of the Poisson and rollover burr [27, 28]. Meanwhile, caused by the Poisson and tear burr, the free surface is observed to be relatively clean with a slight volume of small burrs on one top side as shown in Figs. 5 and 7 [27, 28]. In general, the undesired burrs can be minimized by optimizing the process parameters, mainly including the cutting veloc-ity, feedrate, edge radius, and depth-of-cut [27–29]. However, for the proposed MDC technique, it remains difficult to eliminate the burrs through tuning these parameters, since they are determined based on the requirement for the generation of the specified surface micro/nanostructures. Considering the intricacy of the surface structures, one promising method would be the electron beam irradiation based finishing method for the removal of the burrs [30, 31]. More attentions on the formation mechanism and elimination strategy for the burrs will be paid in future study.

4.2. Generation of a concentric micro-channel

To give a systematic investigation of the MDC technique, a complicated micro/nanofluidic channel consisting of several concentric arcs was fabricated using the same diamond tool and rotational radius. A DoC of 0.8 μm was used, and the machined channel is captured and shown in Fig. 8. The

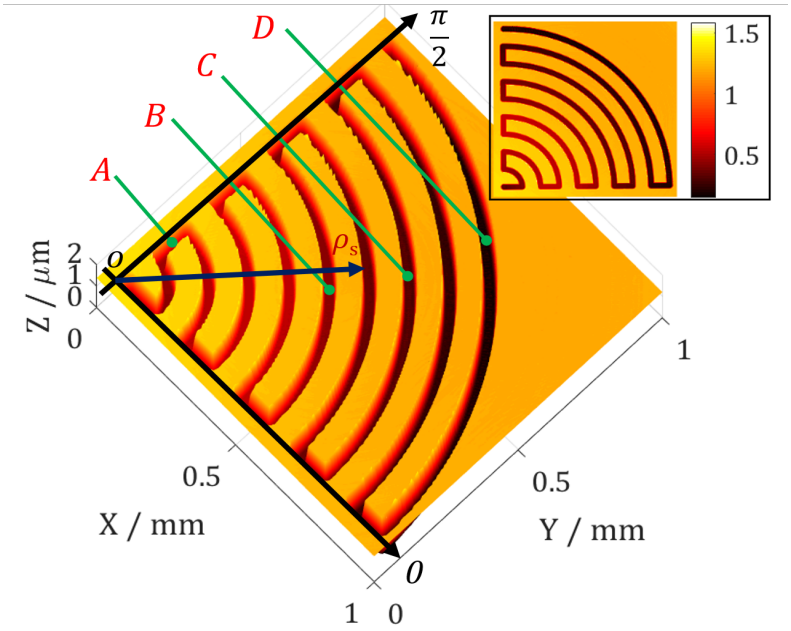

Figure 8: Experimentally generated spiral micro/nanofluidic channel illustrated in its local cylindrical coordinate system.

concentric arcs in the channel are alternately connected at the end points along the radial direction, and the relative radial distance between any two successive arcs is 120 μm. During cutting process, the channel was described in its local cylindrical coordinate system as shown in Fig. 8. The feedrate of the tool for the arc and radial connection channel cutting were set as $\delta = 0.5$ degree and $f = 0.6$ μm per revolution of the spindle, respectively.

Considering the tool shape, the width of the generated micro/nanofluidic channel is measured to be 36 μm, and a high uniformity of features of the micro/nanofluidic channel is observed with a small volume of burrs accumulated at one side on the free surface. In addition, as discussed above, features of the modulated tool marks are highly dependent on the feedrate f which may vary with respect to the polar axis ρ_s for the arc channel cutting in this case ($f = \delta\rho_s$). To show details of the generated surfaces at different positions, the obtained bottom surfaces in regions A, B, C and D as marked in Fig. 8 are extracted and presented in Fig. 9. With the surface in region A (Fig. 9(a)), a super-smooth surface with a surface roughness of $Sa = 1.38$ nm is obtained, attributing to

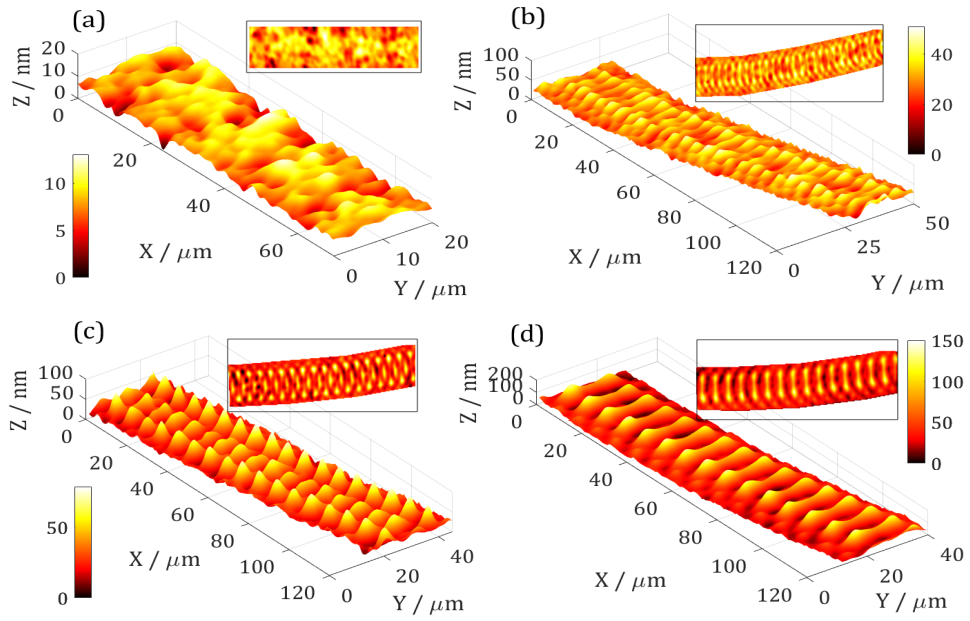

Figure 9: Characteristics of the extracted bottom surface in (a) region A, (b) region B, (c) region C, and (d) region D.

the small feedrate of about 0.6 μm/rev.

With respect to the surface in region B in Fig. 9(b), a slight ripple pattern with two peaks for each structure is observed with a height around 10 nm and periodicity around 4.4 μm, which corresponds to the feeding length. The overall surface roughness with these nano-ripples is about $Sa = 4.05$ nm. In addition, the surface in region C in Fig. 9(c) mainly features a combination of one set of ribbon structures with maximum height around 20 nm and two sets of pyramid structures with maximum height around 40 nm, corresponding to the structures schematically illustrated in regions III and II in Fig. 3, respectively. Region D in Fig. 9(d) is dominated by the hexagonal bulge (region I in Fig. 3) with two peaks at the two ends. The maximum height for the peaks is around 90 nm, and the height at the mid-point of the bulge is around 60 nm. Features of the obtained secondary nanostructures in the four regions exhibit good uniformity. In general, it is foreseeable that micro/nanofluidic channels with different shapes can be generated well through controlling servo motions to follow the desired channel trend.

4.3. Discussion

The proposed MDC technique adopts a basic configuration of a four-axis lathe, whereas it works with a milling kinematics, endowing it with the inherent advantages of micro-milling. Meanwhile, the MDC technique inherits the features of conventional tool servo based turning, and the ultra-fine oscillation of the tool provides it with the capability for efficient generation of complicatedly shaped surfaces. Outperformance of the MDC with respect to turning and micro-milling is summarized as follows:

- Although tool servo based turning is good at generating complicated smooth surfaces, it is commonly hard to fabricate a micro/nanofluidic channel with oriented sharp edges as that obtained in this study. By adopting micro-milling operation through turning kinematics, the MDC gains more flexibility to better adapt to features of the desired micro/nanofluidic channels.

- In micro-milling, it is difficult to adjust the relative position between the tool and the spindle axis with sub-micron accuracy. However, the turning configuration in the MDC enables a much easier alignment of the tool with nanometre accuracy through the applicable tool setting methods, guaranteeing a much higher machining accuracy.

- Limited by the dimensional size of micro milling tools, it is extremely difficult to generate spatially varying shapes with features in dozens of microns through micro-milling. However, a diamond turning tool with motion modulation in the MDC can generate complex features even in the nanoscale, providing much higher machining flexibility.

- With the MDC technique, turning and micro-milling operations can be freely combined for one cutting without any changes of a machining system, leading to a better matching of the structures and optimal cutting strategies. This is significant for the generation of not only

complex micro-channels, but also freeform and micro/nanostructured functional surfaces.

Although the MDC technique is highly flexible for the generation of complex micro/nanofluidic channels, the required frequency and amplitude for the planar modulation motion are highly dependent on the spindle speed and dimensions of the desired channel. Therefore, the achievable size, machining accuracy, and machining efficiency will be inevitably restricted by the moving capability of the two planar slides in terms of the system dynamics behavior.

5. Conclusion

This study provides a new modulated diamond cutting (MDC) technique to generate mi-cro/ nanofluidic channels with spatially-varying shapes. The tri-axial translational servo motions enable the MDC to conduct a more flexible milling operation using a turning configuration, leading to advantages outperforming both turning and micro-milling. Taking advantage of the inherent re-cutting effect, the tool mark modulation by tuning cutting parameters is adopted in the MDC to generate ultra-smooth channel surface as well as to superimpose certain nanostructures on the generated channels. Basic principle of the MDC is detailed and demonstrated by generating certain straight channels through both numerical simulation and experimental cutting. Moreover, a con-centric micro/nanofluidic channel with various superimposed nanostructures on the bottom surface is fabricated.

Acknowledgment

The authors thank the National Natural Science Foundation of China (51705254, 51675455), the Natural Science Foundation of Jiangsu Province (BK20170836), and the Fundamental Research Funds for the Central Universities (30917011301, 309171A8804) for funding.

References

[1] Y. Xu, M. Shinomiya, A. Harada, Soft matter-regulated active nanovalves locally self-assembled in femtoliter nanofluidic channels, Advanced Materials 28 (11) (2016) 2209–2216.

[2] K. S. Elvira, X. C. i Solvas, R. C. Wootton, The past, present and potential for microfluidic reactor technology in chemical synthesis, Nature chemistry 5 (11) (2013) 905.

[3] M. Wang, C. Zhao, X. Miao, Y. Zhao, J. Rufo, Y. J. Liu, T. J. Huang, Y. Zheng, Plasmofluidics: Merging light and fluids at the micro-/nanoscale, Small 11 (35) (2015) 4423–4444.

[4] J. Kim, J. Lee, C. Wu, S. Nam, D. Di Carlo, W. Lee, Inertial focusing in non-rectangular cross-section microchannels and manipulation of accessible focusing positions, Lab on a Chip 16 (6) (2016) 992–1001.

[5] J. Zhou, Y. Wang, L. D. Menard, S. Panyukov, M. Rubinstein, J. M. Ramsey, Enhanced nanochannel translocation and localization of genomic dna molecules using three-dimensional nanofunnels, Nature communications 8 (1) (2017) 807.

[6] T. Yasui, N. Kaji, M. R. Mohamadi, Y. Okamoto, M. Tokeshi, Y. Horiike, Y. Baba, Electroosmotic flow in microchannels with nanostructures, ACS nano 5 (10) (2011) 7775–7780.

[7] X. Chen, L. Zhang, Review in manufacturing methods of nanochannels of bio-nanofluidic chips, Sensors and Actuators B: Chemical 254 (2018) 648–659.

[8] W. Han, P. Hou, S. Sadaf, H. Schäfer, L. Walder, M. Steinhart, Ordered topographically patterned silicon by insect-inspired capillary submicron stamping, ACS applied materials & interfaces 10 (2018) 7451?7458.

[9] J. Shao, Y. Ding, W. Wang, X. Mei, H. Zhai, H. Tian, X. Li, B. Liu, Generation of fully-

covering hierarchical micro-/nano-structures by nanoimprinting and modified laser swelling, Small 10 (13) (2014) 2595–2601.

[10] M. E. Wilson, N. Kota, Y. Kim, Y. Wang, D. B. Stolz, P. R. LeDuc, O. B. Ozdoganlar, Fabrication of circular microfluidic channels by combining mechanical micromilling and soft lithography, Lab on a Chip 11 (8) (2011) 1550–1555.

[11] N. P. Macdonald, J. M. Cabot, P. Smejkal, R. M. Guijt, B. Paull, M. C. Breadmore, Comparing microfluidic performance of three-dimensional (3d) printing platforms, Analytical chemistry 89 (7) (2017) 3858–3866.

[12] H. Gong, B. P. Bickham, A. T. Woolley, G. P. Nordin, Custom 3d printer and resin for 18 μm$\times$ 20 μm microfluidic flow channels, Lab on a Chip 17 (17) (2017) 2899–2909.

[13] S. Waheed, J. M. Cabot, N. P. Macdonald, T. Lewis, R. M. Guijt, B. Paull, M. C. Breadmore, 3d printed microfluidic devices: enablers and barriers, Lab on a Chip 16 (11) (2016) 1993–2013.

[14] N. Bhattacharjee, A. Urrios, S. Kang, A. Folch, The upcoming 3d-printing revolution in microfluidics, Lab on a Chip 16 (10) (2016) 1720–1742.

[15] D. J. Guckenberger, T. E. de Groot, A. M. Wan, D. J. Beebe, E. W. Young, Micromilling: a method for ultra-rapid prototyping of plastic microfluidic devices, Lab on a Chip 15 (11) (2015) 2364–2378.

[16] A. A. Tseng, Removing material using atomic force microscopy with single-and multiple-tip sources, Small 7 (24) (2011) 3409–3427.

[17] Y. Geng, Y. Yan, Y. Xing, X. Zhao, Z. Hu, Modelling and experimental study of machined depth in afm-based milling of nanochannels, International Journal of Machine Tools and Manufacture 73 (2013) 87–96.

[18] T. Gan, X. Zhou, C. Ma, X. Liu, Z. Xie, G. Zhang, Z. Zheng, Liquid-mediated three-dimensional scanning probe nanosculpting, Small 9 (17) (2013) 2851–2856.

[19] J. Zhang, T. Cui, C. Ge, Y. Sui, H. Yang, Review of micro/nano machining by utilizing elliptical vibration cutting, International Journal of Machine Tools and Manufacture 106 (2016) 109–126.

[20] E. Brinksmeier, O. Riemer, R. Gläbe, B. Lünemann, C. Kopylow, C. Dankwart, A. Meier, Submicron functional surfaces generated by diamond machining, CIRP annals 59 (1) (2010) 535–538.

[21] Y.-L. Chen, Y. Cai, K. Tohyama, Y. Shimizu, S. Ito, W. Gao, Auto-tracking single point diamond cutting on non-planar brittle material substrates by a high-rigidity force controlled fast tool servo, Precision Engineering 49 (2017) 253 – 261.

[22] S. To, Z. Zhu, H. Wang, Virtual spindle based tool servo diamond turning of discontinuously structured microoptics arrays, CIRP Annals-Manufacturing Technology 65 (1) (2016) 475–478.

[23] Z. Zhu, S. To, K. F. Ehmann, G. Xiao, W. Zhu, A novel diamond micro-/nano-machining process for the generation of hierarchical micro-/nano-structures, Journal of Micromechanics and Microengineering 26 (3) (2016) 035009.

[24] Z. Zhu, S. To, K. F. Ehmann, X. Zhou, Design, analysis, and realization of a novel piezoelectrically actuated rotary spatial vibration system for micro-/nanomachining, IEEE/ASME transactions on mechatronics 22 (3) (2017) 1227–1237.

[25] M. Hadad, M. Ramezani, Modeling and analysis of a novel approach in machining and structuring of flat surfaces using face milling process, International Journal of Machine Tools and Manufacture 105 (2016) 32–44.

[26] Z. Zhu, S. To, S. Zhang, Theoretical and experimental investigation on the novel end-fly-cutting-servo diamond machining of hierarchical micro-nanostructures, International Journal of Machine Tools and Manufacture 94 (2015) 15–25.

[27] X. Wu, L. Li, N. He, Investigation on the burr formation mechanism in micro cutting, Precision Engineering 47 (2017) 191–196.

[28] K. Lee, D. A. Dornfeld, Micro-burr formation and minimization through process control, Precision Engineering 29 (2) (2005) 246–252.

[29] R. Kobayashi, S. Xu, K. Shimada, M. Mizutani, T. Kuriyagawa, Defining the effects of cutting parameters on burr formation and minimization in ultra-precision grooving of amorphous alloy, Precision Engineering 49 (2017) 115–121.

[30] J. Murray, P. Kinnell, A. Cannon, B. Bailey, A. Clare, Surface finishing of intricate metal mould structures by large-area electron beam irradiation, Precision Engineering 37 (2) (2013) 443–450.

[31] A. Okada, Y. Uno, J. McGeough, K. Fujiwara, K. Doi, K. Uemura, S. Sano, Surface finishing of stainless steels for orthopedic surgical tools by large-area electron beam irradiation, CIRP Annals-Manufacturing Technology 57 (1) (2008) 223–226.

List of Figures

Highlights

1. A novel MDC technique is proposed for the generation of micro/nanofluidic channels;

2. Diamond turning and micro-milling are fundamentally synthesized in the MDC;

3. Motion modulation and tool mark modulation strategies are combined;

4. Micro/nanofluidic channels with complicated shapes and hierarchical structures can be generated.